

# Full Color Display with High Color Stability Obtained by Incorporating Semipolar LEDs and Quantum Dot Photoresist

**Konthoujam James Singh<sup>1</sup>, Yu-Ming Huang<sup>1,2</sup>, Hao-Chung Kuo<sup>1</sup>**

[hckuo@faculty.nctu.edu.tw](mailto:hckuo@faculty.nctu.edu.tw)

<sup>1</sup>Department of Photonics and Graduate Institute of Electro-Optical Engineering, College of Electrical and Computer Engineering, National Yang Ming Chiao Tung University, Hsinchu 30010, Taiwan

<sup>2</sup>Institute of Photonic System, National Yang Ming Chiao Tung University, Tainan 71150, Taiwan

Keywords: Quantum dot photoresist, semipolar  $\mu$ -LEDs, wide color gamut.

## ABSTRACT

We demonstrated red-green-blue (RGB) full-color micro light emitting diodes ( $\mu$ -LEDs) using quantum dot photoresist color conversion layer. With a peak wavelength shift of 3.2 nm and a 14.7% efficiency droop under 200 A/cm<sup>2</sup> injected current density, the semipolar  $\mu$ -LEDs show a significant improvement in the quantum-confined Stark effect. The RGB pixel displayed a low color shift with current density and had a wide color gamut of 114.4% NTSC and 85.4% Rec. 2020.

## 1 Introduction

Owing to many performance advantages over common-use technologies, micro light emitting diodes ( $\mu$ -LEDs) are the promising candidate for next generation display technology [1-4]. Red-green-blue (RGB)  $\mu$ -LEDs can be assembled to achieve full color displays using mass transfer process; however, there are still some challenges in terms of low transfer yield, slow throughput and high manufacturing cost [5,6]. To overcome these challenges, color conversion based on quantum dots (QDs) which requires a blue or UV-LEDs as pumping source is adopted but commercial UV-LEDs are grown on c-plane sapphire substrate [7]. GaN based LEDs grown on c-plane substrates suffer from efficiency droop caused by quantum confined Stark Effect (QCSE) resulting from polarization related electric field [8,9]. GaN is a hexagonal crystal with a structure of wurtzite symmetry, the highest structure consistent with spontaneous piezoelectric polarization. Owing to spontaneous and piezoelectric polarization, as c-plane-grown GaN materials are subject to high built-in electric fields. LEDs based on c-plane epitaxial wafers can only work at low current densities as the current density increases due to the substantial decrease in efficiency. A better way to reduce this is to address the origin of the crystal plane's polarization field, so growing LED devices on semipolar planes is a well-known approach to droop reduction [10,11]. The followings are the details about the file format, the composition, and the text contents in the manuscript.

Colloidal quantum dots (QDs) is suitable to use as a color conversion layer for  $\mu$ -LEDs, and a high contrast ratio can be achieved with QD-based  $\mu$ -LED displays [12,13]. Photolithography technique can be used for producing high-resolution  $\mu$ -LED display and also to overcome the

challenges faced in mass transfer process [14,15]. QDs can be combined with photoresist (PR) to form QDPR and this approach will provide a way to pattern QDPR arrays that can monitor size and thickness while maintaining the photolithography benefits. This technique produces the bottlenecks with a cost-effective, realistic solution in developing high-resolution, large-area devices, particularly full-color  $\mu$ -LEDs for display applications. In this work, full-color  $\mu$ -LED array is fabricated using semipolar (20-21) blue LEDs with a 50 $\mu$ m diameter chip size and a green or red QDPR color-conversion layer. This is the evidence that the semipolar  $\mu$ -LED system innovatively achieves full-color display and comparing to c-plane LEDs, semipolar LEDs show much better wavelength shift characteristics and improved efficiency droop. In addition, the use of photoresist matrix helps in achieving high contrast and more color stability of  $\mu$ -LED.

## 2 Experiment

Metal-organic chemical vapor deposition (MOCVD) can be used to grow (20-21) oriented GaN layer on patterned sapphire substrate (PSS). The conventional way of growing semipolar GaN by off-axis slicing of bulk-form GaN substrate grown by hybrid vapor-phase epitaxy is expensive and not desirable for mass production. To address this problem an advanced orientation-controlled epitaxy (OCE) method was used to directly grow GaN material on the sapphire wafer, which is a simple epitaxy method involving MOCVD to produce semipolar GaN. The epitaxial structure of the semipolar device consisted of a bulk GaN buffer layer (5  $\mu$ m), an n-GaN layer (1.5  $\mu$ m), an undoped InGa<sub>0.15</sub>N/GaN MQW active layer, a p-GaN layer (150 nm), and a p-InGa<sub>0.15</sub>N layer (3 nm). The MQWs were designed using five pairs of 3 nm thick InGa<sub>0.15</sub>N wells and a 5 nm thick GaN barrier with a wavelength of about 450 nm on emission. In this analysis, the c-plane wafer was also developed with a similar MQW structure. Then  $\mu$ -LED array was formed using 200 nm thick SiO<sub>2</sub> as passivation layer deposited by plasma-enhanced chemical vapor deposition technique. Later, lithographic process is used to deposit black photoresist (PR) matrices and QDPR on the semipolar  $\mu$ -LED array and a black photoresist (PR) was

used to flatten the array to prevent lateral leakage of blue light. Next, the lithography process sequentially produced the gray photoresist, red QDPR, green QDPR, and transparent PR to form a color pixel on a highly transparent glass substrate and this color pixel on glass was stuck together with  $\mu$ -LED.

### 3 Results and Discussion

A large-area semipolar GaN is grown on a patterned sapphire substrate using the orientation-controlled epitaxy as mentioned in the above section. The optical and electrical properties of the fabricated  $\mu$ -LEDs have been characterized in this section. Fig. 1(a) displays the electroluminescence (EL) spectrum at different current densities showing a wavelength peak at 453 nm and full width at half maximum (FWHM) of 24.8 nm under 200 A/cm<sup>2</sup> injection current density. This narrow FWHM suggests that the epitaxy offers a high quality structure and is therefore responsible for the delivery of purer emitted light, matching colors and color gamut distribution.

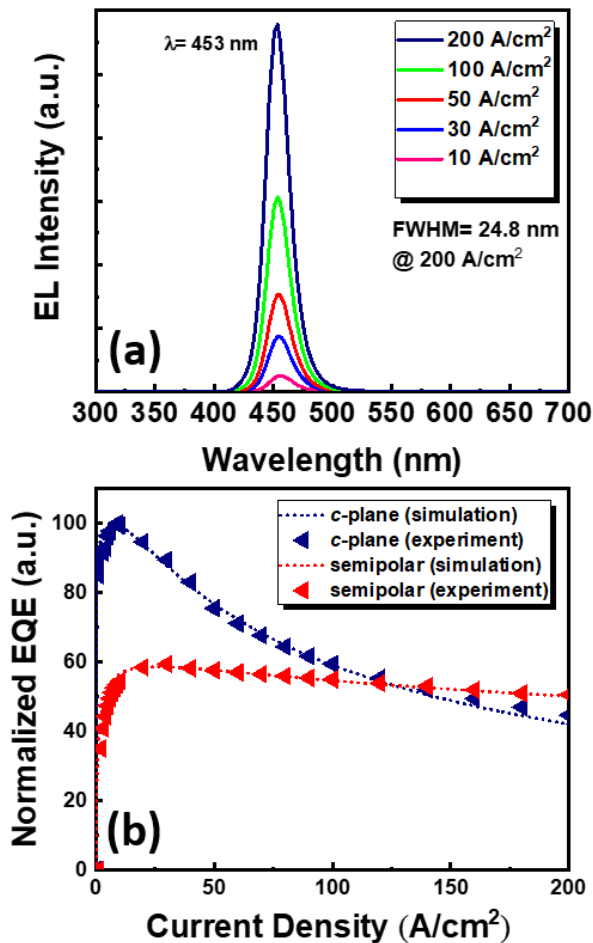


Fig. 1 (a) EL spectrum of semipolar  $\mu$ -LED. (b) Simulated and experimental EQE for semipolar and c-plane  $\mu$ -LEDs.

Fig. 1(b) gives the experimental data as well as simulation fit for the external quantum efficiency for both c-plane and semipolar devices. It can be seen from figure that the

simulation fit and the experimental data has a good agreement and the c-plane device has a larger EQE than that of semipolar device. Despite having a lower EQE, the output power of semipolar device is sufficient for the application of color conversion. In addition, the semipolar device shows an efficiency drop of just 14.7% at a high injection current density of 200 A/cm<sup>2</sup> while the c-plane device shows a 55% drop in efficiency under the same conditions. It is suggested that the output power and the EQE can be further improved by optimizing the active area of the device. The severe efficiency drop in c-plane devices can be explained by two important phenomena i.e. carrier leakage and Auger recombination, which will cause QCSE leading to low carrier recombination rate. The polarization charges that accumulate at the hetero interfaces of the active region can also induce tilting of the energy band and can separate the overlap of the wave-function distribution resulting in nonradiative recombination and carrier leakage.

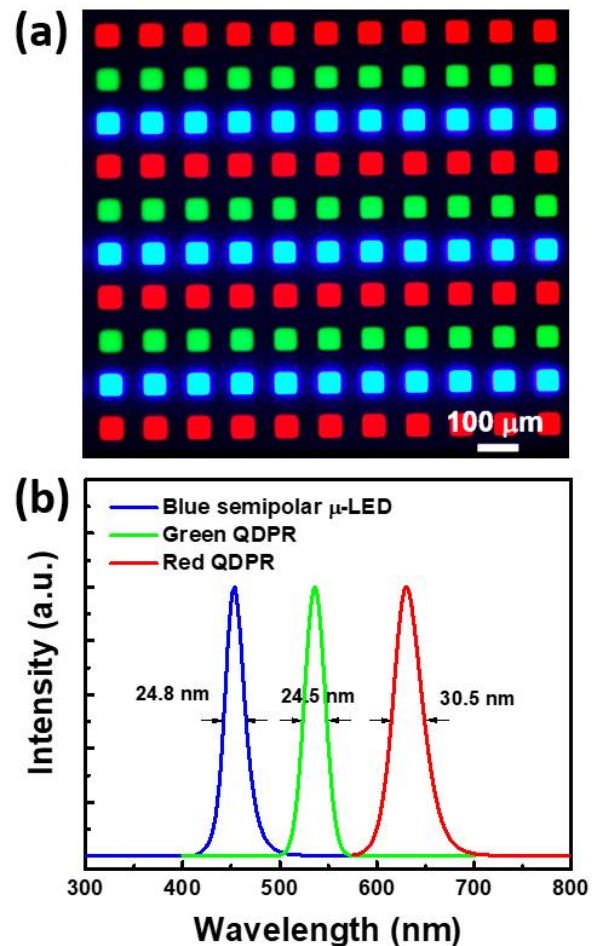
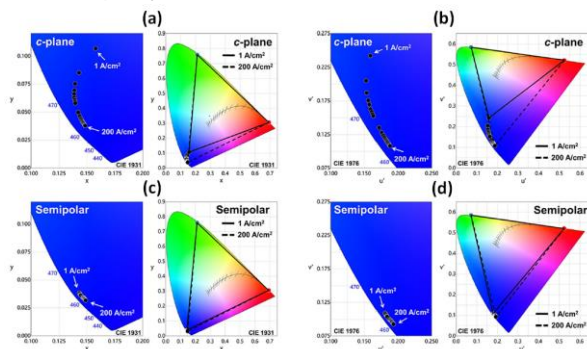


Fig. 2 (a) Fluorescence microscopy image of RGB pixel. (b) EL spectrum for blue  $\mu$ -LED, green and red pixel.

Fig. 2(a) represents the fluorescence microscopy (FLOM) image of RGB pixel matrices on glass showing a high contrast ratio between the gray PR matrices and the color pixels. The gray PR can exhibit higher

reflectivity as compared to the black PR thereby reducing the cross-talk effect between the pixels and increasing the output intensity by inside reflection. Fig. 2(b) represents the EL spectra of semipolar blue  $\mu$ -LED, green and red pixels showing peak wavelengths of 453 nm, 536 nm and 630 nm respectively. The corresponding FWHM for the RGB emission spectra are 30.5 nm, 24.5 nm and 24.8 nm, hence these narrow FWHMs specify good performance in color rendering. It is clear that the blue light leakage has been reduced by using QDPR and it can be further reduced by increasing the thickness of QDPR or changing its composition. Since blue light leakage is minimized, only blue light from QD pixel remains, and each pixel will independently show brilliant colors. Hence, red and green QDPR pixels can filter blue light and significantly enhance the color purity.



**Fig. 3 (a) CIE 1931 and (b) CIE 1976 diagram for c-plane  $\mu$ -LED and QDPR. (c) CIE 1931 and (d) CIE 1976 diagram for semipolar  $\mu$ -LED and QDPR.**

The color performance of the RGB  $\mu$ -LEDs under the injection current density from 1 A/cm<sup>2</sup> up to 200 A/cm<sup>2</sup> is demonstrated in Fig. 3 using CIE 1976. The color coordinates for c-plane device vary from (0.1572, 0.1067) to (0.1483, 0.0379) and for semi-polar device, the variation is from (0.1433, 0.0388) to (0.1490, 0.0317) in CIE 1931 chromaticity diagram. It is found that the color shift ( $\mu'u'$ ) for semipolar blue  $\mu$ -LEDs i.e. 0.0209 is smaller than that of c-plane which is 0.1374 in CIE 1976. The color gamut of the RGB made from semipolar  $\mu$ -LED is almost unchanged when the current density of the injection increases, although there is a variation of about 10% under the same conditions for c-plane device. Also, the red and green pixels display no color shift due to emission by optical pumping and stability of QDPR. The RGB pixel fabricated using semipolar  $\mu$ -LED and QDPR shows a wide-color gamut by achieving 114.4% of National Television Standards Committee (NTSC) space and 85.4% Rec. 2020 in the CIE 1931. Hence, the RGB pixels produced using semipolar  $\mu$ -LED and QDPR show excellent color stability and wide color gamut characteristics responsible for next generation display applications.

## 4 Conclusions

In the concluding remarks, RGB full color  $\mu$ -LED device has been fabricated from semipolar  $\mu$ -LEDs and QDPR using lithography process. The semipolar  $\mu$ -LED grown on PSS is inexpensive and can provide good epitaxial quality. The semipolar  $\mu$ -LED demonstrates wavelength stability by giving a wavelength shift of 3.2 nm while c-plane  $\mu$ -LED exhibits a shift of 13 nm. Also the semipolar device shows a lower efficiency droop of only 14.7% under high injection current density of 200 A/cm<sup>2</sup> as compared to c-plane device. Finally the RGB pixels display a wide color gamut of 114% NTSC and 85.4% Rec. 2020 with high color stability by showing a very small color shift.

## References

- [1] Liu, Zhitian, et al. "Efficient single-layer white light-emitting devices based on silole-containing polymers." *Journal of Display Technology* 9.6 (2013): 490-496.
- [2] Gong, Z., et al. "Efficient flip-chip InGaN micro-pixelated light-emitting diode arrays: promising candidates for micro-displays and colour conversion." *Journal of Physics D: Applied Physics* 41.9 (2008): 094002.
- [3] Wu, Tingzhu, et al. "Mini-LED and micro-LED: promising candidates for the next generation display technology." *Applied Sciences* 8.9 (2018): 1557.
- [4] Tan, Guanjun, et al. "High dynamic range liquid crystal displays with a mini-LED backlight." *Optics Express* 26.13 (2018): 16572-16584.
- [5] Zhang, Lei, et al. "Wafer-scale monolithic hybrid integration of Si-based IC and III-V epi-layers—A mass manufacturable approach for active matrix micro-LED micro-displays." *Journal of the Society for Information Display* 26.3 (2018): 137-145.
- [6] Cok, Ronald S., et al. "Inorganic light-emitting diode displays using micro-transfer printing." *Journal of the Society for Information Display* 25.10 (2017): 589-609.
- [7] Han, Hau-Vei, et al. "Resonant-enhanced full-color emission of quantum-dot-based micro LED display technology." *Optics Express* 23.25 (2015): 32504-32515.
- [8] Takeuchi, Tetsuya, et al. "Quantum-confined Stark effect due to piezoelectric fields in GaInN strained quantum wells." *Japanese Journal of Applied Physics* 36.4A (1997): L382.
- [9] Takeuchi, Tetsuya, et al. "Determination of piezoelectric fields in strained GaInN quantum wells using the quantum-confined Stark effect." *Applied Physics Letters* 73.12 (1998): 1691-1693.
- [10] Feezell, Daniel F., et al. "Semipolar (20-2-1) InGaN/GaN light-emitting diodes for high-efficiency solid-state lighting." *Journal of Display Technology*

9.4 (2013): 190-198.

- [11] Masui, Hisashi, et al. "Nonpolar and semipolar III-nitride light-emitting diodes: Achievements and challenges." *IEEE Transactions on Electron Devices* 57.1 (2009): 88-100.
- [12] Achermann, Marc, et al. "Nanocrystal-based light-emitting diodes utilizing high-efficiency nonradiative energy transfer for color conversion." *Nano Letters* 6.7 (2006): 1396-1400.
- [13] Erdem, Talha, and Hilmi Volkan Demir. "Color science of nanocrystal quantum dots for lighting and displays." *Nanophotonics* 2.1 (2013): 57-81.
- [14] Park, Joon-Suh, et al. "Alternative patterning process for realization of large-area, full-color, active quantum dot display." *Nano Letters* 16.11 (2016): 6946-6953.
- [15] Keum, Hohyun, et al. "Photoresist contact patterning of quantum dot films." *ACS Nano* 12.10 (2018): 10024-10031.